Journal of the Korean Nuclear Society
Volume 16, Number 2, June, 1984

A Study on the Reactivity Effect due to Expansion of Diagrid and Pad

Young In Kim, Keun Bae Oh, Kun Joong Yoo, and Mann Cho

Korea Advanced Energy Research Institute

(Received March 31, 1984)

Diagrid와 Pad의 팽창에 의한 반응도 효과에 대한 연구

김영인 · 오근배 · 유건중 · 조 만

한국에너지연구소

(1984. 3. 31 접수)

Abstract

With the help of the nuclear computational system for a large LMFBR (KAERI-26 group cross section library/1DX/2DB), the reactivity coefficients for the diagrid expansion and the pad expansion at the beginning of cycle of the equilibrium core of SUPER-PHENIX I are calculated and reviewed. The core is described using R-Z geometry model, and a two-dimensional multigroup diffusion theory is used. For reference cases, reactivity calculations for radial and axial uniform expansion are performed, and also calculated are reactivity variations due to changes in material density and core volume. The reactivity coefficient for the diagrid expansion is calculated to be −0.553pcm/mil. The temperature coefficient corresponding to the above value is −1.0766pcm/°C and is well in accord with the French datum of −1.09pcm/°C within 1.2% difference. With the use of the calculational method for the diagrid expansion effect, reactivity calculations for the pad expansion bringing about nonuniform expansion are performed, which show that the calculational method is very useful in the analysis of the pad expansion effect. The reactivity coefficients for the pad expansion are calculated to be −0.2743 pcm/mil and −0.2786pcm/mil for the averaged expansion model and for the integrated pancake model, respectively. Under the assumption of the free expanding core the temperature reactivity coefficients for each model are obtained to be −0.5766pcm/°C and −0.5858pcm/°C, both of which agree with the French datum of −0.574pcm/°C within 2% difference.

요 약

대형 고속증식로용 핵계산 체제(KAERI-26군 단면적 library/1DX/2DB)를 이용하여 SUPER-PHENIX I 평형 노심의 초기상태에서의 diagrid 및 pad팽창에 대한 반응도 계수를 계산, 검토하였다. 노심은 R-Z등가 model로 묘사하고, 2차원 다군 확산 이론 전산코드인 2DB를 사용하여 임계도를 계산하였다.

기초계산으로서 반경방향 및 축방향 균일 팽창에 대한 반응도 계산과 노심구성물질의 원자수 밀도

변화와 노심체적 변화에 대한 반응도 변화량계산을 수행하였다. 균일 팽창으로 고려한 diagrid팽창에 대한 반응도 계수는 −0.553pcm/mil로 계산되었다. 한편 반응도의 온도계수는 −1.0766pcm/°C로 환산되어 프랑스 발표치 −1.09pcm/°C와 1.2%오차내로 일치하였다. Diagrid 팽창효과 계산방법을 활용하여 노심의 불균일 팽창을 유발하는 pad팽창에 대한 반응도 계수 계산을 수행한 바 매우 유용함을 알았다. Pad 팽창에 대한 반응도 계수는 평균팽창 model의 경우 −0.2743pcm/mil, pancake집적 model의 경우 −0.2786pcm/mil로 각각 계산되었다. 또한 자유팽창 노심에서의 온도변화에 따른 pad 팽창에 대한 반응도 계수는 각 model에 대하여 −0.5766pcm/°C, −0.5858pcm/°C로 계산되어 프랑스 발표치 −0.574pcm/°C와 2% 오차내로 일치하였다.

1. Introduction

A liquid metal fast breeder reactor(LMFBR) operates at high temperature and has a large temperature difference between core inlet and outlet, as compared to an LWR or an HWR. In the case of SUPER-PHENIX I in which sodium is used as the coolant, the average coolant temperature is about 470°C while that in an LWR or an HWR is about 280°C∼300°C. And the temperature difference of coolant between core inlet and outlet is about 150°C in SUPER-PHENIX I while that in an LWR or an HWR is below 40°C. Also, an LMFBR has a temperature margin in excess of 300°C between the operating temperature and the boiling point of sodium. Therefore, core deformation due to the large temperature difference may occur in an LMFBR during normal operation as well as transients. Thermal expansion changes the geometry and the density of the material of the core. This, in turn, affects the reactivity of the system. In general, thermal expansion decreases the material density of the core, which brings about the negative reactivity effect, while the increase of the volume of the core represents the positive reactivity effect.

The thermal expansion effects for the reactivity can be, in the main, divided into two effects as follows: First, the diagrid expansion effect in which the diagrid and the core expand uniformly due to the rise of inlet coolant temperature. Second, the pad expansion effect in which the upper part of the core expands more than the lower part in such cases as the primary pump coastdown and overpower transient where the temperature difference between the core inlet and outlet becomes larger than that at normal operation owing to the decrease of the heat removal capacity.

Other effects due to the temperature change in an LMFBR are as follows: Doppler effect due to fuel temperature rise, control rod insertion effect due to different temperature rise between control rod drive system and reactor vessel, sodium voiding effect, and sodium density effect. As a result, the temperature rise effects in an LMFBR play an important role in safety analysis, and it would be of great use in enhancement of safety if the reactivity insertion effect is effectively utilized by giving adequate temperature margins.

In this paper the diagrid expansion effect and the pad expansion effect, as the negative reactivity effects, have been calculated for the beginning of cycle (BOC) of equilibrium core of a larges cale LMFBR, SUPER-PHENIX I, and these results have been compared with the French data. At first, reactivity coefficients for uniform axial core expansion, uniform radial core expansion, and uniform radial and axial core expansion were calculated. Then the reactivity coefficients for the diagrid expansion effect and the pad expansion effect have been obtained using these uniform expansion reactivity coefficients. The calculational method of the diagrid expansion effect has been introduced in the

calculation of the pad expansion effect, employing the averaged expansion model and the integrated pancake model.

The nuclear computational system for a large LMFBR(KAERI-26 group cross section library[1] /1DX[2]/2DB[3]) has been used in this calculation and the reactivity effects will be produced by the direct k_{eff} calculation method.

2. Calculational Models and Methods

2-1. Calculational Model

The Bondarenko format 26 group constant data are generated from the evaluated nuclear data file ENDF/B-IV[4], using the ETOX-K4[5]. The PUPX program applies energy self-shielding factors and provides the corrected cross sections to the 1DX program. The 1DX program computes and applies fine flux weighting factors to account for the heterogeneous distributions of materials. The homogeneous resonance self-shielding cross sections are subsequently used in the 2DB(two-dimensional multigroup diffusion) program.

The R-Z geometry model for the beginning of cycle(BOC) of equilibrium core of SUPER-PHENIX I shown in Figure 1, was chosen to describe the axial and radial core configuration. In this model, material densities for each region are selected from the KAERI report.[6] And the geometrical data of assemblies are given in Table 1.

Generally in computing reactivity coefficients, the Δk_{eff} calculation method with diffusion theory or the reactivity calculation method with perturbation theory can be used.[7] In this study, the Δk_{eff} calculation with 2DB diffusion code was used for the calculation of reactivity coefficients.

The assumptions used in this study are as follows:

—Core is free to expand.

—The structural material temperature of the core is equal to the coolant temperature.

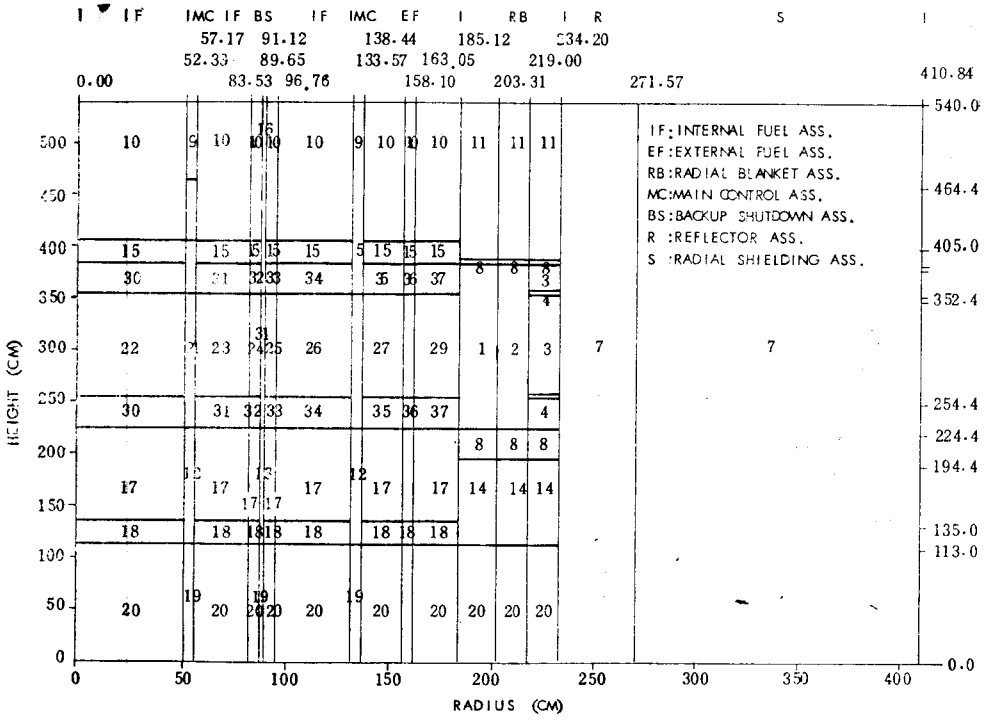

Fig. 1. R-Z Geometry Medel with All Control Rods Out for the Core of SUPER-PHENIX I

Table 1. Geometric Design Features of Assemblies

Assembly	Fuel Assembly	Radial Blanket Assembly
Assembly Number	193/171 (Inner/Outer)	233
Fuel Pins per Assembly	271	91
Length(mm)	5,400	5,400
Duct, Across Flats(mm)		
Inside	163.8	163.8
Outside	173.0	173.0
Fuel Pin		
Length(mm)	2,700.0	1,944.0
Cladding O.D. (mm)	8.5	15.8
Pin Piteh(mm)	9.8	16.87
Fuel Diameter(mm)	7.0	14.5
Length of PuO_2-UO_2 Region(mm)	1,000	
Length of UO_2 Region (mm)	300×2	1,600
Wire Diameter(mm)	1.2	0.95
Wire Pitch(mm)	300	200

—The radial temperature distribution at a given axial level is uniform.

—The amount of sheath expansion of hexagonal assembly is equal to that of assembly expansion.

—The sum of the amounts of expansion of an assembly corresponds to the amount of expansion of the core at a given axial level.

—The total mass of core material is constant regardless of core expansion.

2-2. Calculational Methods

The calculational procedure using the R-Z model is shown in Figure 2, where main parameters calculated in each step are also illustrated. In accordance with the calculational procedure, reactivity calculations for uniform expansion are performed with calculation of volume change according to temperature change, and from these calculations the temperature reactivity coefficients both for the diagrid expansion effect and the pad expansion effect are finally obtained.

2-2-1. Reactivity Change Due to Uniform Expansion Effect

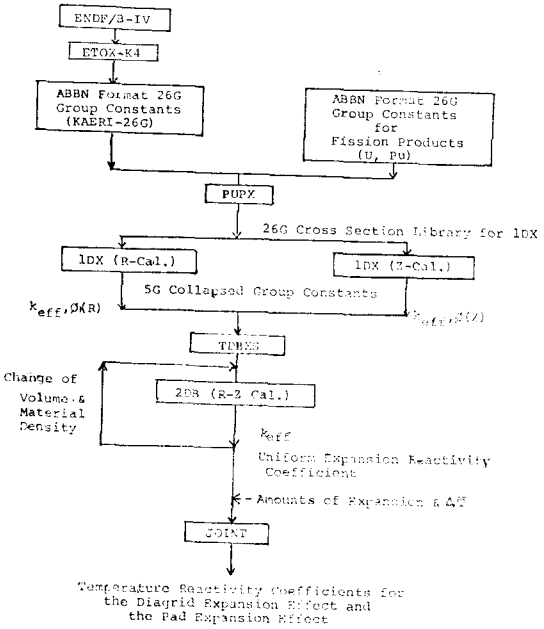

Fig. 2. Schematic Diagram for Calculational Procedure

Reactivity calculations due to uniform expansion effect are carried out for preparation of basic data to be used in further calculations of the diagrid expansion effect and the pad expansion effect considering the material density change as well as volume change, and at this time the total mass of core is kept constant. Since the total mass of the core remains constant, densities of all the materials included within the core are considered to be decreased with the volume expansion of the core.

The amount of uniform expansion is obtained using Eqs. (1) and (2).[8]

$$\Delta R = R\alpha_c(T_c - 298) \quad \cdots\cdots(1)$$

$$\Delta H = H\alpha_c(T_c - 298) \quad \cdots\cdots(2)$$

where R is a radius and H a height of core at room temperature of 25°C. And where α_c is the mean linear thermal expansion coefficient for type 316 stainless steel as follow;

$$\alpha_c(T_c) = 1.789\times10^{-5} + 2.398\times10^{-9}T_c + 3.269\times10^{-13}T_c^2 \quad \cdots\cdots(3)$$

where T_c is the average structure temperature °K

Reactivity changes due to uniform expansion are given by

$$\Delta\rho=\frac{k_{eff}-1}{k_{eff}}-\frac{k^0_{eff}-1}{k_{eff}{}^0}$$

$$=\frac{1}{k^0_{eff}}-\frac{1}{k_{eff}} \quad (4)$$

where k^0_{eff} is an effective multiplication factor for the standard core with no deformation and k_{eff} that for a deformed core.

2-2-2. Reactivity Change Due to Actual Expansion Effect

Diagrid Expansion Effect

Diagrid is a lower supporting structure of the core, through which coolant flows into assemblies. As the dimension of the diagrid is radially changed with increase in the inlet coolant temperature, each assembly expands uniformly and the intervals between them also increase due to diagrid radial expansion. After calculating the amounts of diagrid expansion according to rising of inlet coolant temperature, the reactivity coefficient for the diagrid expansion effect is obtained, using the results which have been previously determined.

Amounts of diagrid expansion according to temperature change, ΔR_{dia}, can be determined as below;

$$\Delta R_{dia}=2342.01\ \alpha_c(\bar{T}_{dia})(\bar{T}_{dia}-298) \quad (5)$$

where 2342.01mm is the $R-Z$ equivalent core diameter to radial blanket and $\bar{T}_{dia}(^0K)$ an average temperature of diagrid. From results of Eq. (5), fractional volume changes in diagrid expansion are calculated and reactivity changes in accordance with fractional changes are obtained.

Next to it, the temperature reactivity coefficient for the diagrid expansion effect, $(\rho_T)_{dia}$, can be computed with the use of Eq. (6),

$$(\rho_T)_{dia}=\frac{\Delta\rho_2-\Delta\rho_1}{\Delta T_2-\Delta T_1} \quad (6)$$

where $\Delta\rho_1, \Delta\rho_2$ are reactivity changes, and ΔT_1, ΔT_2 temperature rises for each state of 1 and 2, respectively.

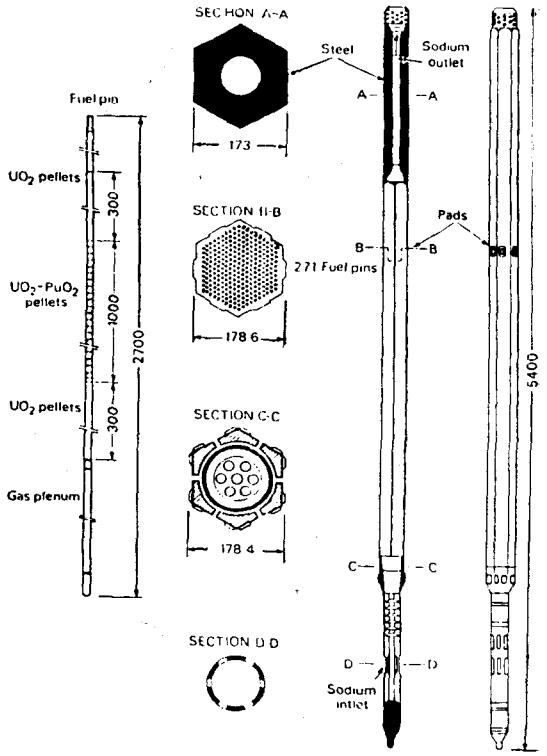

Fig. 3. Sectional Diagrams of Fuel Assembly

Pad Expansion Effect

The clearance between assemblies at room temperature is 6mm. Each face of the wrapper tube is provided with a pad which locally reduces the clearance between assemblies to 0.4mm at room temperature as shown in Figure 3.[9]

The pads are located on the boundary between upper axial blankets and gas plenums, and consequently it is reasonable to assume that temperature of structural material at the pad level is equivalent to that of outlet coolant temperature.

Amounts of expansion at the pad level, ΔR_{pad}, can be calculated using the following Eq.(7), which has been derived by considering a clearance between assemblies of 0.4mm,

$$\Delta R_{pad}=2336.78\ \alpha_c\ (\bar{T}_{pad})(\bar{T}_{pad}-298)$$
$$-5.23 \quad (7)$$

where 2336.78mm is the diameter of structures

excluding clearances 5.23mm the sum of clearances, and both values have been obtained from converting actual dimensions of structures into $R-Z$ equivalent diameters.

Then amounts of relative expansion at the pad level compensating the amount of diagrid expansion can be given by

$$\Delta R_{rel}=\Delta R_{pad}(\bar{T}_{pad})-\Delta R_{dia}(\bar{T}_{dia}) \cdots\cdots\cdots (8)$$

From solutions of Eq. (8), it is concluded that the temperature difference between diagrid and pads, (ΔT), of 107°C brings pads into contact during raising of power from hot zero power to hot full power, and that the pad expansion effect takes place only if ΔT exceeds 107°C.

Here one comes across the problem such as how to describe the core deformations due to the differential thermal expansion, utilizing the given two dimensional calculation system. In other words, since contacts between pads transform the core into a flowering shape, a three-dimensional calculation should be carried out to make a detailed reactivity calculation for the flowering-shaped core. In order to apply the two-dimensional calculation system as shown in Fig. 1, two models are adopted in the description of the flowering-shaped core as follows;

A) An averaged expansion model

An averaged expansion model is a calculational method, through which amounts of core deformation due to the expansion effect are converted into those of uniform core expansion, and reactivity changes are calculated in the same way as the calculation of the diagrid expansion effect using the converted amounts.

B) An integrated pancake model

An integrated pancake model is an another attempt, which describes the deformed core as an integrated pancake form. In this model the core is divided into six pancakes, i.e., two for upper and lower axial blanket region, and four for fuel region, and modelized as a six pancakes-integrated shape. Pancakewise expansion rates are determined to linearly increase from the lower axial blanket region with the assumption that the expansion rate of the upper axial blanket region is equivalent to that of the pad level. In addition, the followings are considered in the calculation of the pad expansion effect;

1) The total reactivity change due to the pad expansion effect can be expressed as the sum of pancakewise reactivity changes, which are proportional to its axial contribution factor ($f_{\alpha i}$) for uniformly expanded core having the same expansion rate. Pancakewise axial contribution factors are determined from the calculation of reactivity worths by the perturbation of local density.

2) Pancakewise volume fractions are corrected into those of the uniformly expanded core having the expansion rate at the pad level by introducing a volume correction factor.

Following the above assumptions, reactivity changes due to the pad expansion effect can be calculated by

$$(\Delta\rho)_{total}=\sum_{i=1}^{6}\Delta\rho(\alpha_i)\cdot f_{\alpha i}\cdot W_i \cdots\cdots\cdots (9)$$

where $\Delta\rho(\alpha_i)$, $f_{\alpha i}$ and W_i are a reactivity change according to the expansion rate α_i, a volume correction factor, and an axial contribution factor for pancake i, respectively.

And $\Delta\rho(\alpha_i)$ can be given as below;

$$\Delta\rho(\alpha_i)=-\rho_\alpha\cdot\alpha_i \cdots\cdots\cdots\cdots\cdots\cdots (10)$$

where ρ_α (pcm/(% of expansion)) is an expansion reactivity coefficient. The volume correction factor, $f\alpha_i$, can be expressed as

$$f\alpha_i=\frac{V\alpha_6}{V\alpha_i}=\frac{(1+\frac{\alpha_6}{100})^3}{(1+\frac{\alpha_i}{100})^3} \cdots\cdots\cdots (11)$$

The averaged expansion model and the integrated pancake model are employed to calculate reactivity changes due to the pad expansion effect, and temperature reactivity coefficients for the pad expansion effect, $(\rho_T)_{dia}$, are finally obtained in the same way as Eq. (6).

3. Results and Discussion

3-1. Uniform Expansion Reactivity Coefficient

Figure 4 shows the k_{eff} change for the uniform expansion in radial, axial, and radial-axial directions of the core. Table 2 also shows the reactivity changes according to the uniform expansion. k_{eff} and the reactivity are linearly varied as shown in Figure 4 and Table 2, and the calculated reactivity coefficients are -438.75 pcm/(% of radial expansion), -76.26 pcm/(% of axial expansion), and -505.87 pcm/(% of radial and axial expansion).

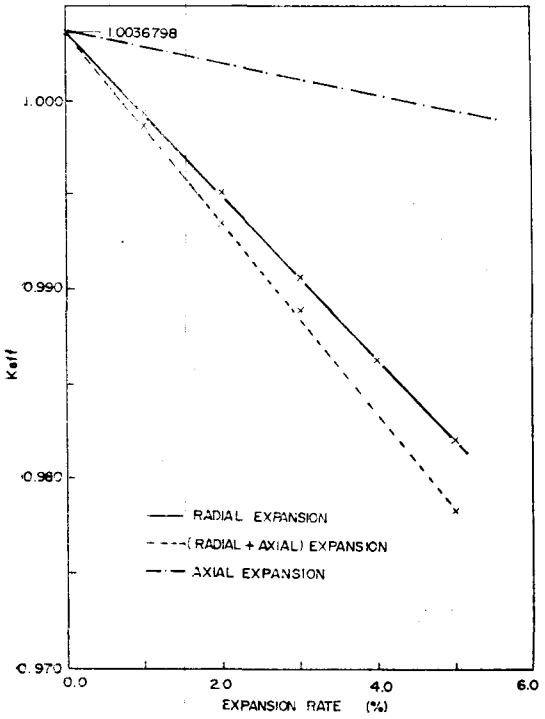

Fig. 4. k_{eff} Changes with Uniform Expansion

The above results represent the effects due to changes in volume and material density. In case of the volume effect and the material density effect, the reactivity coefficients of +81.51 pcm/(% of volume increase) and of −265.23 pcm/(% of decrease of material density) are calculated. This means that the effect of the change of the material density acts more than three times as much as that of the change of the volume does in the uniform expansion effect.

3-2. Diagrid Expansion Effect

Table 3 shows the amount of expansion, the expansion, the expansion rates, and the reactivity changes according to the temperature changes from 395°C up to 600°C in diagrid.

The reactivity coefficient due to the dimensional changes of the diagrid is calculated to be -0.553 pcm/mil. Employing the relationship between changes in volume and temperature, the temperature reactivity coefficient corresponding to the above value is converted to be −1.766 pcm/°C and is well in accord with the French published value[10] of −1.09 pcm/°C which is within 1.2% difference. According to the above results, the decrease of reactivity of 367.77 pcm has been obtained, resulting from the dimensional change of diagrid in hot full power condition.

3-3. Pad Expansion Effect

Table 4 shows the amounts of pad expansion

Table 2. Ractivity Changes for Uniform Expansion

Expansion Form / Expansion Rate(%)	Radial		Radial+Axial	
	k_{eff}	$\Delta\rho$(pcm)	k_{eff}	$\Delta\rho$(pcm)
0	1.0036798		1.0036798	
1	0.99938503	−428.17	0.99868198	−498.61
2	0.99504998	−864.10	0.99350330	−1,020.55
3	0.99072601	−1,369.32	0.98894664	−1,484.32
4	0.98636217	−1,749.27	0.98361065	−2,032.87
5	0.98200794	−2,198.80	0.97827466	−2,587.41

Table 3. Reactivity Changes according to $\Delta\bar{T}_{inlet}$(Diagrid Expansion Effect)

$\bar{T}_{dia}$(°C)	$\Delta\bar{T}_{inlet}$(°C)[1]	$(\Delta R)_{dia}$(mm)	$(\Delta R/R)_{dia}$(mm)	$\Delta\rho$(pcm)
395	0	17.02	0.727	−367.77[2]
450	55	19.70	0.841	−425.45
500	105	22.18	0.947	−479.07
550	155	24.70	1.054	−533.20
600	205	27.25	1.163	−588.34

Notes: 1) $\Delta\bar{T}_{inlet}(°C)=\bar{T}_{dia}-395$ 2) Reactivity changes due to expansion in HZP

Table 4. Amounts of Expansion according to $\Delta\bar{T}$[1]

$\bar{T}_{pad}$(°C)		$\Delta\bar{T}$(°C)	$(\Delta R)_{dia}$(mm)	$\left(\frac{\Delta R}{R}\right)_{dia}$(%)	$(\Delta R)_{pad}$(mm)	$\left(\frac{\Delta R}{R}\right)_{pad}$(%)	$\left(\frac{\Delta R}{R}\right)_{rel}$(%)[2]
395	500	105	17.017	0.7266	16.656	0.7112	—
	502	107[3]			17.001	0.7259	0.0000
	545	150			19.158	0.8180	0.0914
	595	200			21.699	0.9265	0.1999
	645	250			24.278	1.0366	0.3100
	695	300			26.893	1.1483	0.4217
	745	350			29.547	1.2616	0.5352
	795	400			32.239	1.3766	0.6500
	845	450			34.970	1.4932	0.7666
	895	500			37.741	1.6115	0.8849

Notes: 1) $\Delta\bar{T}(°C)=\bar{T}_{pad}-395$; temperature difference between the core inlet and outlet

2) $\left(\frac{\Delta R}{R}\right)_{rel}(\%)=\left(\frac{\Delta R}{R}\right)_{pad}-\left(\frac{\Delta R}{R}\right)_{dia}$

3) Temperature difference that brings pads into contact

Table 5. Factors Considered in the Integrated Pancake Model

Item \ Pancake(i)		1	2	3	4	5	6
Expansion Rate (α_i) (%)		α_1	α_2	α_3	α_4	α_5	α_6
$\Delta\bar{T}$(°C)[1]	150	0.7266	0.7477	0.7653	0.7828	0.8005	0.8180
	250	0.7266	0.7981	0.8578	0.9174	0.9770	1.0366
	350	0.7266	0.8501	0.9530	1.0558	1.1587	1.2616
	450	0.7266	0.9035	1.0509	1.1984	1.3458	1.4923
	500	0.7266	0.9307	1.1008	1.2709	1.4409	1.6115
Volume Correction Factor[2]		f_{α_1}	f_{α_2}	f_{α_3}	f_{α_4}	f_{α_5}	f_{α_6}
$\Delta\bar{T}$(°C)[1]	150	1.0027	1.0021	1.0016	1.0010	1.0005	1.0
	250	1.0093	1.0071	1.0053	1.0035	1.0018	1.0
	350	1.0160	1.0123	1.0092	1.0061	1.0031	1.0
	450	1.0230	1.0176	1.0132	1.0088	1.0044	1.0
	500	1.0266	1.0204	1.0152	1.0101	1.0050	1.0
Axial Contribution Factor(w_i)		0.0671	0.1879	0.2742	0.2728	0.1854	0.0126

Note: 1) $\Delta\bar{T}=\bar{T}_{pad}-395$ 2) $f_{\alpha_i}=\dfrac{\left(1+\frac{\alpha_6}{100}\right)^3}{\left(1+\frac{\alpha_i}{100}\right)^3}$ for $i=1,\ldots,6$

according to the temperature differences between the core inlet and outlet in the equilibrium core. As shown in Table 4, the pads are brought into contact when the temperature difference between the diagrid and the pad reaches 107°C. Table 5 shows the expansion rates, the volume fractions, the volume correction factors, and the axial contribution factors for the integrated pancake model described in the preceding section.

The pancakewise axial contribution factors in Table 5 are obtained from the axial reactivity worth map due to density change, which is shown is in Figure 5.

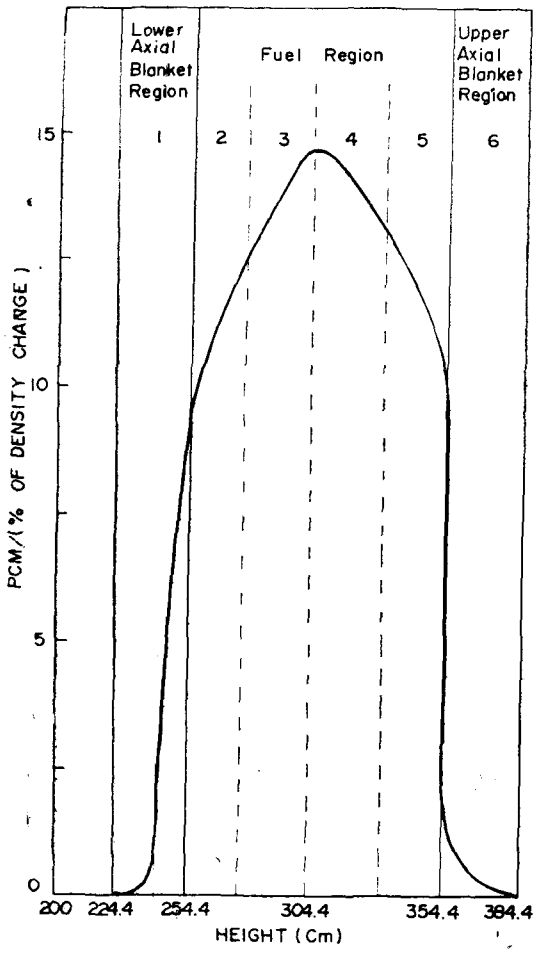

FIG. AXIAL REACTIVITY WORTH MAP

Fig. 5. Axial Reactivity Worth Map

Table 6. Reactivity Changes according to $\Delta\bar{T}$[1] (Pad Expansion Effect) (Unit: pcm)

$\Delta\bar{T}$(°C)[1] \ Model	Averaged Expansion Model	Integrated Pancake Model
150	−390.69	−390.73
250	−445.98	−446.31
350	−502.90	−503.71
450	−561.48	−562.59
500	−591.40	−593.83
Reactivity Coefficient (pcm/mil)	−(0.2743± 0.0001)	−(0.2786± 0.0045)
Reactivity Coefficient (pcm/°C)	−(0.5766± 0.0171)	−(0.5858± 0.0253)

Note: 1) $\Delta\bar{T}=\bar{T}_{pad}-395$

The reactivity changes and the reactivity coefficients for each model for the pad expansion effect are shown in Table 6, where the reactivity coefficients due to the dimensional changes of the core at the pad level are calculated to be −0.2743 pcm/mil for the averaged expansion model and −0.2786 pcm/mil for the integrated pancake model.

As shown in Table 6, the temperature reactivity coefficients for the pad expansion effect are also obtained to be −0.5766 pcm/°C and −0.5858 pcm/°C, respectively, under the assumption of the free expanding core model. It is recommended that the analysis of the pad expansion effect should be carried out by the method which can describe the mechanical behavior of the core more precisely than that of the free expanding core model.

4. Conclusions

The results show that the calcualtional methods are very useful in the analyses of the diagrid expansion effect and the pad expansion effect.

Especially it is noticeable that both the diagrid concept and the pad concept are still adopted in the conceptual design of the RNR

1,500 Project, which had been already initiated by the European Cooperation.[11] Therefore it is thought that the calculational methods can be effectively used in the analyses of the diagrid expansion effect and the pad expansion effect in future large commercial fast breederr eactors such as RNR 1,500MWe.

References

1. J.D. Kim and J.T. Lee, "Generation of 26 Group Constant Library for Fast Reactor Calculations," KAERI/RR-288/81(1982).
2. R.W. Hardie and W.W. Little, Jr., "1DX, A One-Dimensional Diffusion Code for Generating Effective Nuclear Cross Sections," BNWL-954, Battle Memorial Institute Pacific Northwest Laboratory (1969).
3. W.W. Little, Jr. and R.W. Hardie, "2DB, A Two-Dimensional Diffusion-Burnup Code for Fast Reactor Analysis," BNWL-640, Battle Memorial Institute Pacific Northwest Laboratory (1968).
4. D. Garber, et al., "Data Formats and Procedures for the Evaluated Nuclear Data File, ENDF," BNL-NCS-50456 (Oct. 1975).
5. J.D. Kim and J.T. Lee, "ETOX-K4, A Code to Calculate Group Constants for Nuclear Reactor Calculations," KAERI/TR-34/81.
6. M. Cho, et al., "A Study on the Core Characteristics of the Fast Breeder Reactor," KAERI/RR-374/82 (1983).
7. W. Mayo and R.A. Doncals, "Reactivity Feedback Coefficients for Use in CRBR Transient Analyses," Advanced Reactors, Physics, Design, and Economics, pp. 688-698, Pergamon Press (1975).
8. L. Leibowtz, E.C. Chang, M.G. Chasanov, R.L. Gibby, C. Kim, A.C. Millunzi, and D. Stahl, "Properties for LMFBR Safety Analysis," ANL-CEN-RS-76-1, Argonne National Laboratory (March 1976).
9. M. Banel, et al., "Construction of the World's First Full Scale Fast Breeder Reactor," *Nucl. Eng. Int.*, **23**, No. 273, 43-60 (June 1978).
10. H. Noel, et al., "Analysis of the Dynamic Behavior of the Phenix and Super-Phenix Reactors During Certain Accident Sequences." Proc. Int. Meeting on Fast Reactor Technology, Seattle (Aug. 1979).
11. "Project Rapide 1,500MW," EdF(Jan. 1984).